Helena NOWAKOWSKA

Institute of Fluid Flow Machinery, Polish Academy of Sciences, Gdańsk
ORCID: 0000-0002-6342-1596

doi:10.15199/48.2022.05.04

Effect of discharge tube properties on parameters of surface-wave sustained plasma

Streszczenie. *Zbadano numerycznie wpływ promienia wewnętrznego i zewnętrznego, przenikalności elektrycznej i temperatury rury wyładowczej na współczynniki propagacji i tłumienia fali elektromagnetycznej oraz temperaturę gazu, temperaturę i gęstość elektronów w mikrofalowym wyładowaniu podtrzymywanym falą powierzchniową o częstotliwości 2,45 GHz w argonie pod ciśnieniem atmosferycznym. Do obliczeń wykorzystano dwutemperaturowy model plazmy i założenie o lokalnej osiowej jednorodności wyładowania.*

Abstract*. The effects of inner and outer radius, permittivity and discharge tube temperature on electromagnetic wave propagation and attenuation coefficients, as well as gas temperature, electron temperature and density in a microwave discharge sustained by a surface wave in argon at 2.45 GHz were numerically investigated. A two-temperature plasma model and the assumption of local axial uniformity of the discharge were used for the calculations. (**Wpływ właściwości rury wyładowczej na parametry plazmy mikrofalowej wytwarzanej przez falę powierzchniową**).*

Słowa kluczowe: fala powierzchniowa, plazma mikrofalowa, wyładowanie mikrofalowe, parametry plazmy.
Keywords: surface wave, microwave plasma, microwave discharge, plasma parameters.

Introduction

Microwave surface-wave (SW) sustained discharges have been studied for decades, since effective devices for their generation such as the surfatron [1] and surfaguide [2], were invented. They have found many applications, especially since they began to be applied to gases at atmospheric pressure. They have been used for gas processing [3], surface treatment [4], and more recently for hydrogen production [5] graphene fabrication [6], CO_2 reduction [7] or as plasma antennas [8]. They are generated in dielectric tubes by the electric field of an electromagnetic wave propagating along the dielectric-plasma interface. In such a structure, the plasma column is created by the wave, while being the medium that allows the wave to propagate. Surface-wave discharges (SWDs) are efficient, very stable and can be produced over a wide range of pressures, electromagnetic field frequencies and absorbed powers. A characteristic feature of SWDs is that increasing the power delivered to the discharge increases the length of the plasma column and the radially averaged electron density $n_{e,a}$ decreases along the plasma column almost linearly. Since the slope of $n_{e,a}$ along the plasma axis is almost constant, this gives the effect of 'pushing out' the plasma column from the plasma source with increasing the delivered power. In other words, a plasma column viewed from its end has the same properties regardless of the absorbed power and column length. A detailed description of SWDs properties can be found in the review [9].

The main goal of experimental studies on the SWDs was to find distributions of the electron density n_e and temperature T_e, gas temperature T_g and concentration of excited states depending on the gas pressure p, wave frequency f and the discharge tube internal radius a. It has been found that the slope of radially averaged electron density increases as the wave frequency and gas pressure increase, and as the tube inner radius a decreases [9, 10]. The subject of the research was also the wave propagation characteristics, i.e. the dependence of the phase β and attenuation α coefficients on plasma parameters.

In theoretical works, the same relationships as well as electric field $\mathbf{E}$ distributions and the influence of selected electron collisions and chemical reactions on plasma parameters were studied. Typically, however, these were studies of single relationships rather than full, systematic studies of the effects of various parameters. The goal of the modeling was to obtain agreement between computational and experimental results for given discharge conditions. An exception were articles [11, 12], in which the effect of discharge tube radii and material on axial electron density profiles was systematically investigated. These early studies were related to low-pressure discharges, which are easier to model than atmospheric-pressure discharges. This is due to the fact that in the former the gas temperature can be treated as constant. In the latter, the electron density is higher, and the frequency of electron collisions with gas particles ν is greater than the wave angular frequency ω, which causes more intense energy transfer to the gas, and thus stronger gas heating.

Contemporary self-consistent models take into account many plasma species, and the number of collisions and chemical reactions is impressive [13-15]. Their agreement with experimental results is very good. However, their computational cost is very high, so they are performed for specific discharge conditions, and there is no systematic study of the effect of discharge conditions on plasma parameters such as the electron or gas temperature.

In this paper, effect of the discharge parameters, namely the inner and outer radii, electric permittivity and temperature of the discharge tube on distributions of the electron density and temperature, gas temperature, wave phase and attenuation coefficients is systematically studied. Two-temperature (2T) plasma model and local axial uniformity approximation (LAUA) in cylindrical coordinate system is adopted. It allows for separate determination of the radial and axial distributions of plasma parameters, which are next properly connected. LAUA is valid if the plasma column length is much larger than its radius, because then the axial gradients can be neglected, as they are much smaller than the radial ones [13, 16]. 2T model with LAUA is widely used in modelling both low and atmospheric pressure SWDs [13, 17, 18]. It significantly speeds up the computation and allows for efficient parametric studies. The model neglects gas flow, so for high flow rates the results may differ from those obtained experimentally or from fully self-consistent models, but for low gas flows their agreement with experiment is good and they correctly reflect the typical regularities [13, 18].

Calculations presented here are performed for argon at atmospheric pressure, axially symmetric SWD and wave frequency 2.45 GHz. The results give insight into the behavior of the discharges, facilitate the analysis of experimental results and make it easier to optimize them.

Model description

The model is presented in a simplified way, because the details are presented in different works [13, 17-19]. The radial distributions of the plasma parameters (T_e, T_g and n_e) are determined from the equations of conservation of the electron energy, gas energy and electron density number, which have the form, respectively:

$$(1)\quad \frac{1}{r}\frac{\mathrm{d}}{\mathrm{d}r}\left(r\lambda_e\frac{\mathrm{d}T_e}{\mathrm{d}r}\right)+\frac{1}{2}\sigma\mathbf{E}^2-\frac{3}{2}\delta\nu n_e k_B(T_e-T_g)=0$$

$$(2)\quad \frac{1}{r}\frac{\mathrm{d}}{\mathrm{d}r}\left(r\lambda_g\frac{\mathrm{d}T_g}{\mathrm{d}r}\right)+\frac{3}{2}\delta\nu n_e k_B(T_e-T_g)=0$$

$$(3)\quad \frac{1}{r}\frac{\mathrm{d}}{\mathrm{d}r}\left(rD_{amb}\frac{\mathrm{d}n_e}{\mathrm{d}r}\right)+S_{CR}n_e n_a-\alpha_{CR}n_e n_i=0$$

where r is the radial coordinate, λ_g and λ_e are the gas and electron thermal conductivities, respectively, σ is the plasma electrical conductivity, $\mathbf{E}$ is the electric field phasor, δ is the fraction of electron energy lost in a collision with a gas particle, ν is the effective frequency of electron elastic collisions, k_B is the Boltzmann constant, D_{amb} is the ambipolar diffusion coefficient, S_{CR} and α_{CR} are the ionization and recombination coefficients, respectively, n_a and n_i are the concentrations of atoms and ions, respectively. The method of determining these parameters for argon and boundary conditions used is given in [19].

The radial electric field distributions are determined from the wave equation

$$(4)\quad \nabla^2\mathbf{E}+\frac{\omega^2}{c^2}\varepsilon_r\,\mathbf{E}=0$$

where c is the speed of light in vacuum, ε_r is the relative permittivity of a medium and $\omega=2\pi f$.

These radial distributions are determined as a function of L – the linear density of the wave power absorbed in plasma defined as

$$(5)\quad L=2\pi\int_0^a\frac{1}{2}\sigma(r)\mathbf{E}^2(r)r\mathrm{d}r\ .$$

The attenuation and phase coefficients are calculated from the dispersion equation taking into account the conditions of continuity of the respective field components of the interfaces between the plasma, discharge tube and surrounding air, as described in [9].

The axial distribution of the power absorbed in plasma $L(z)$ (where z is the axial coordinate) can be found from [18]

$$(6)\quad \frac{\mathrm{d}L(z)}{\mathrm{d}z}=-2\alpha(L)L(z)\left[1-\frac{L(z)}{\alpha(L)}\frac{\mathrm{d}\alpha(L)}{\mathrm{d}L}\right]^{-1}$$

by solving it with the boundary condition $L(d) = L_{\alpha\beta}$, where d is the position of the plasma column end and $L_{\alpha\beta}$ is the value of L for which the condition defining the plasma end ($\alpha = \beta$) is met. Knowing the distribution of $L(z)$ and the radial distributions of the plasma parameters, depending for given discharge conditions only on L, one obtains the full 2-D structure of the discharge.

Results

All calculations were performed in MATLAB® environment. Typical calculation results obtained from the model are presented in Fig. 1. They show spatial distributions of the gas temperature T_g, electron temperature T_e and electron density n_e, for a = 1 mm, outer discharge tube radius b = 2 mm, the relative permittivity of the tube ε_d = 3.78 (as for fused silica) and the tube wall temperature T_w = 900 K (this quantity is used as a boundary condition for (2)). Since the solution is axially symmetric, only a half of the radial distribution is shown, with r within 0 and a range. The axial distributions are presented as a function of $z - d$, which is a common convention in SWDs modeling. In the presented case, d = 25 cm, which is a typical length for the applied microwave power.

It can be seen that in each cross section of the tube, the maximum of the gas temperature T_g is on the tube axis and decreases towards the tube wall, where it is 900 K. The value on the axis decreases towards the end of the plasma column. The maximal value is about 2480 K. The electron temperature T_e is higher than the gas temperature in each point. This shows that the plasma is in a state of non-equilibrium. T_e varies from about 8500 K near the end of the plasma column to about 9700 K in the $z - d$ = – 25 cm cross section. The decrease of T_e towards the wall is monotonic near the column end. The distribution becomes almost flat further from the end, and at the beginning of the plasma column, the maximum T_e is near the tube wall. This is a well-known phenomenon associated with the skin effect.

The electron density n_e is maximal on the tube axis and decreases towards the tube wall. Its value on the axis decreases towards the end of the column. The maximum value on the axis is approximately 1.2×10^{21} m^{-3}. The presented properties of the SWD are in a qualitatively good compliance with calculation from self-consistent models [13, 20].

The agreement with the experimental results is also satisfactory, as can be seen in Fig. 2, where the axial distributions of plasma parameters are shown. The experimental results usually present radially averaged values; therefore the calculation results are also averaged. The following formula is used for averaging the electron density:

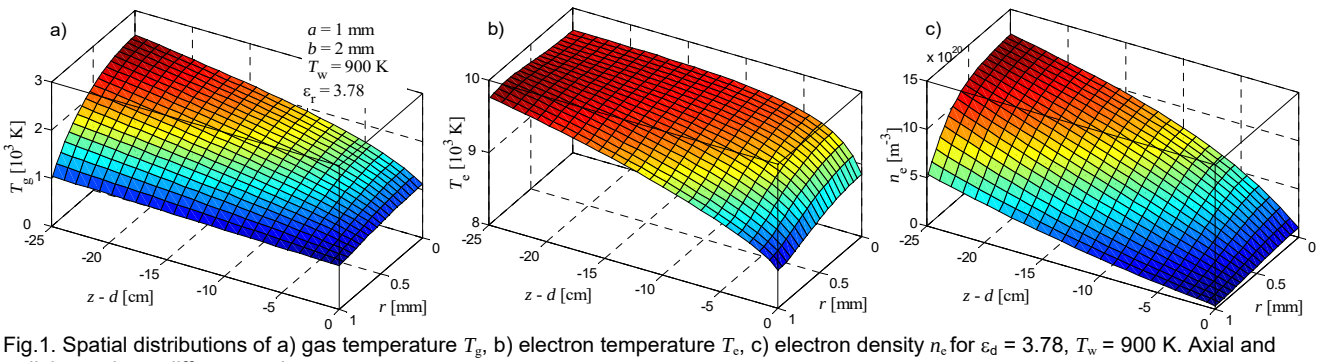

Fig.1. Spatial distributions of a) gas temperature T_g, b) electron temperature T_e, c) electron density n_e for ε_d = 3.78, T_w = 900 K. Axial and radial axes have different scales

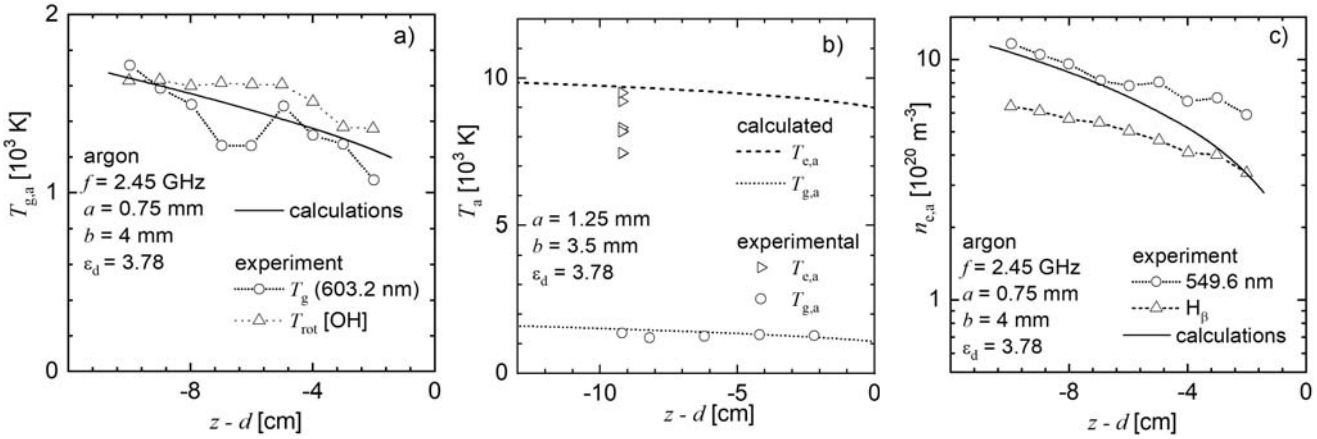

Fig.2. Comparison of experimental and calculated axial distributions of radially averaged: a) gas temperature $T_{g,a}$, [21], b) electron and gas temperature $T_{e,a}$, $T_{g,a}$ [22], c) electron density $n_{e,a}$ [21]

(7) $$n_{e,a} = \frac{1}{\pi a^2}\int_0^a 2\pi\, n_e(r) r \mathrm{d}r \ .$$

The remaining averaged values are derived from analogous formulas.

The calculated averaged gas temperature (Fig. 2a) agrees very well with the experimental results obtained using two spectroscopic methods. The calculated electron temperature is higher than that obtained spectroscopically from different emission lines (Fig. 2b), however the compliance is quite good taking into account that the definitions of this temperature as well as its measurement method may differ [22]. For example, in [23], $T_{e,a} \cong 16$ kK for a = 1 mm, b = 3 mm, which is it is much higher than that shown in Fig. 2b for a tube with very similar radii. The agreement between the gas temperatures for this case is very good. The calculated electron density is higher than that obtained from H_β line (a standard method for determining electron density) but lower than that found from the 549.6 nm ArI line. The higher calculated slope may be partly due to neglect of the gas flow.

Effect of the discharge tube inner radius a on the discharge parameters. Figs. 3a and 3b show the effect of the discharge tube inner radius a (varying from 0.5 mm to 1.5 mm) on SW propagation characteristics. Calculations were done for tubes of relative permittivity ε_d = 3.78 and wall thickness $b - a$ = 1 mm. A relatively small range of changes a was chosen, due to the fact that for an SWD in argon at atmospheric pressure in tubes with a > 1.5 mm, the phenomenon of filamentation, i.e. division of the plasma column into separate plasma filaments, is observed [24,25]. The presented model does not take into account this phenomenon.

As can be seen, for each tube the wave attenuation coefficient α decreases with increasing L. It is an approximate power relationship $\alpha \sim L^x$, where the exponent x is a negative number. For a fixed value of the power density L, the wave attenuation coefficient α decreases with increasing the inner radius a.

The phase coefficient β decreases monotonically with the linear power density L. For L > 300 Wm^{-1}, it weakly depends on L and its value is about 60 m^{-1}, which corresponds to the wavelength λ of about 10.5 cm. For a fixed value of L, β is greater for a tube with a smaller radius a. For L < 300 Wm^{-1}, the coefficient β increases strongly when L decreases. The condition $\alpha = \beta$, defining the plasma column end, is met for $L \cong 150$ Wm^{-1} in each case.

Fig. 3c presents the axial distribution of the linear power density L, obtained from (6). This dependence is almost linear, which is a result of the power dependence of $\alpha(L)$. The value of L increases with decreasing of a. The dependence $L(z)$ enables finding axial and space distributions of all the plasma parameters.

Figs. 3d, 3e and 3f show the axial distributions of the radially averaged gas temperature $T_{g,a}$, electron temperature $T_{e,a}$, and electron density $n_{e,a}$, respectively. It can be seen that $T_{g,a}$ in each case decreases along the plasma column. For the tube with radius a = 0.5 mm, it decreases from about 2400 K to about 1000 K over a length of 30 cm. The change in $T_{g,a}$ along the column is smaller if the radius a is greater. $T_{e,a}$ varies weakly along the plasma column and it increases when the radius a decreases in a selected cross-section. At a distance of 30 cm from the plasma column, $T_{e,a}$ is about 11 kK in a tube with radius a = 0.5 mm and about 10 kK in a tube with radius a = 1.5 mm.

The axial distributions of the averaged electron density are shown in Fig. 3f. A well-known fact can be seen that the averaged electron density decreases almost linearly along the plasma column for all cases [9, 26]. The values of the electron density strongly depend on the radius of the discharge tube: the smaller the radius a, the higher the average electron density in a tube selected cross section.

From Fig. 3 it results that increasing the inner radius of the tube (with the tube thickness constant) causes decreasing of the electron density (which was demonstrated in many experiments) but also gas and electron temperatures.

Effect of the discharge tube outer radius b on the discharge parameters. To evaluate the effect of the tube outer radius b on the plasma parameters, calculations were performed for a tube with the inner radius a = 1 mm, made of a dielectric with the relative permittivity ε_d = 3.78 and four values of the outer radius b (1 mm, 2 mm, 4 mm, 8 mm). The obtained results are shown in Fig. 4. As can be seen, the value of b has a significant impact on the SW propagation characteristics: the thicker the dielectric layer surrounds the plasma, the stronger the effect of this dielectric on the surface wave propagation. The attenuation coefficient α – for a fixed L – increases with the increase of b. For L = 2000 Wm^{-1}, it is $\alpha \cong 2$ m^{-1} in a thin-walled tube ($a = b$) and $\alpha \cong 5$ m^{-1} in a tube with b = 8 mm. In all cases the dependence of $\alpha(L)$ is roughly a power function. The phase coefficient β also strongly depends on the value of b. For a thin-walled tube and L in range from 200 to 2000 Wm^{-1}, $\beta \cong 53$ m^{-1}, which corresponds to $\lambda \cong 12$ cm. For a thick-walled tube (b = 8 mm), $\beta \cong 80$ m^{-1}, i.e. $\lambda \cong 8$ cm. It is seen the presence of such a tube shortens the wavelength by 1.5 times.

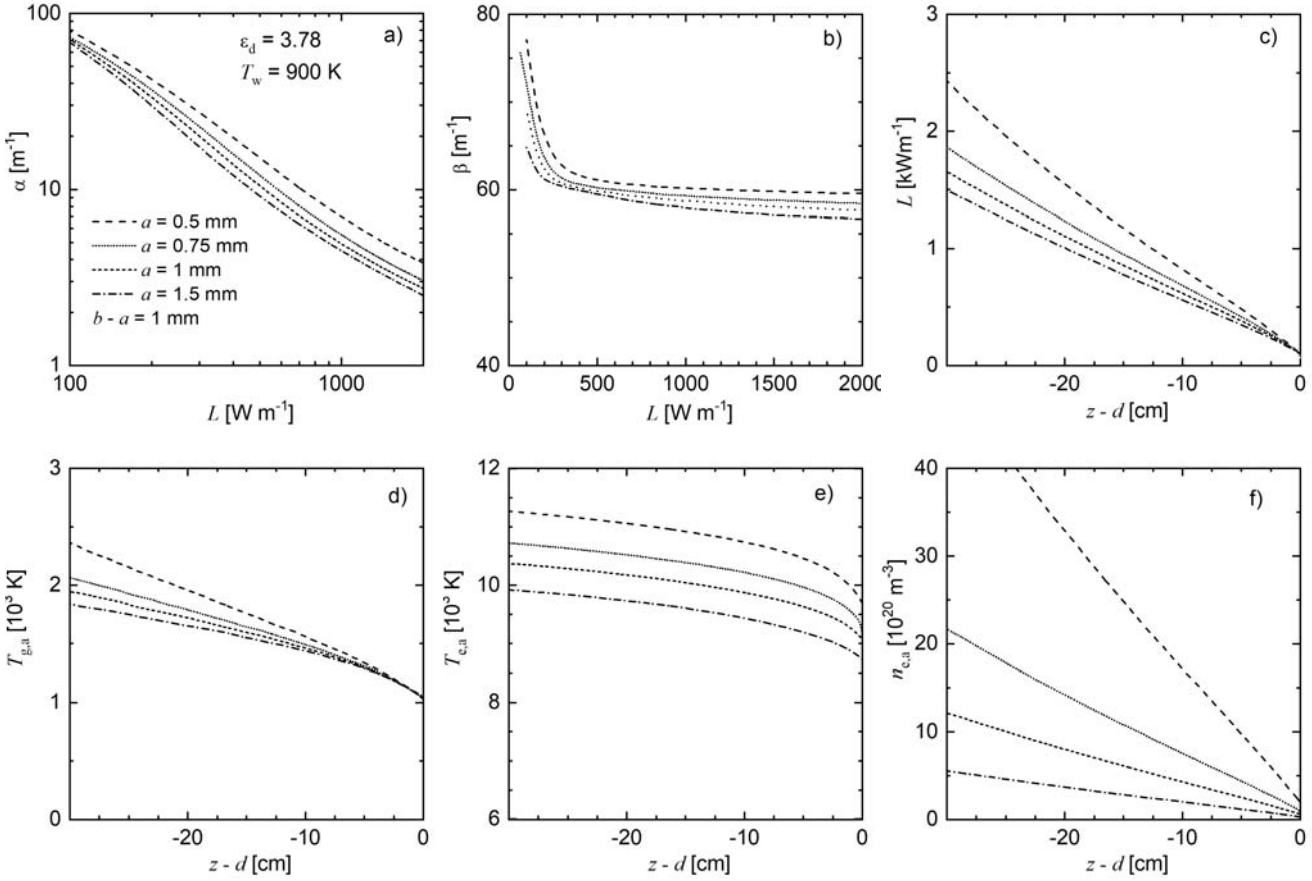

Fig.3. Influence of the discharge tube inner radius a on: a) SW attenuation characteristics $\alpha(L)$; b) SW phase characteristics $\beta(L)$; c) axial distribution of L, d) axial distributions of the average gas temperature $T_{g,a}$, e) average electron temperature $T_{e,a}$, f) average electron density $n_{e,a}$; T_w = 900 K, ε_d = 3.78, $b - a$ = 1 mm

The change of L along the plasma column can be seen in Fig. 4c. It decreases almost linearly and its value increases with increasing the outer radius b. This radius also affects the averaged gas $T_{g,a}$ and electron $T_{e,a}$ temperatures as well as electron density $n_{e,a}$, which is seen in Figs. 4d, 4e and 4f, respectively. While this radius has a weak effect on $T_{e,a}$, its effect on $T_{g,a}$ and $n_{e,a}$ is significant. In all cases, an increase in outer radius causes an increase in the analyzed parameter value. The influence of the outer tube radius on the plasma parameters is not obvious and in some experimental works only the inner radius is given without specifying the outer radius value. However, as can be seen from Fig. 4e it has a strong influence on the electron density slope, which is due to the fact that the presence of a dielectric around the plasma modifies the SW propagation significantly (see Fig 4a). From the comparison of Figs. 3 and 4, it can be seen that increasing the inner radius of the tube has the opposite effect than increasing its outer radius. Therefore, the simultaneous increase of them may give the effect of no impact of these quantities on plasma parameters, in particular for gas and electron temperatures, as it was seen in [27].

Effect of the permittivity of a discharge tube on the discharge parameters. The calculations were made for a tube with the inner radius a = 1 mm, outer radius b = 3 mm and for four values of the relative permittivity of the discharge tube material: ε_d = 1, 2, 4 and 9. These values are close to the typical values used in experiments (e.g. air, quartz and alumina). Figs. 5a and 5b show that the change in ε_d has an influence on the propagation characteristics of the surface wave. The attenuation coefficient α – for a fixed value of L – increases with the increase of the value ε_d. For L = 2000 Wm^{-1}, the attenuation coefficient α in a tube with a permittivity of ε_d = 1 (this is equivalent to a thin-walled tube or plasma surrounded only by air) is approximately 2 m^{-1}, while in a tube for which ε_d = 9, it is almost 4 m^{-1}. The phase coefficient β also depends on the value of ε_d. For plasma surrounded by air (equivalent to the tube permittivity ε_d = 1) in the L value range from 300 to 2000 Wm^{-1}, $\beta \cong$ 53 m^{-1} (this corresponds to $\lambda \cong$ 12 cm). For a tube of the permittivity ε_d = 9, this coefficient is greater, $\beta \cong$ 65 m^{-1}, and the wavelength is shorter ($\lambda \cong$ 9.7 cm). For ε_d = 1 and 2, β decreases monotonically with the increase of L. For ε_d = 4 and 9, the dependence is not monotonic. The range where β grows with the increase of L corresponds to the backward wave [12]. As can be seen from Fig 5c, the greater the value of ε_d, the greater is the linear power density L absorbed in the plasma in the selected tube cross-section and greater the curve slope.

Figs. 5d, 5e and 5f show the axial distributions of the averaged gas temperature, electron temperature and electron density, respectively, depending on the permittivity of the discharge tube ε_d. It can be seen that the increase of ε_d from 1 to 9 slightly increases the electron temperature. The increase in ε_d is accompanied also by an increase in gas temperature (Fig. 5d) and an increase in the electron density (Fig. 5e) in a selected cross-section of the tube. It has long been known that increasing the permittivity of a tube increases the electron density slope and values [28]. However, to our knowledge, the influence of this parameter on the gas and electron temperatures has not been analyzed so far.

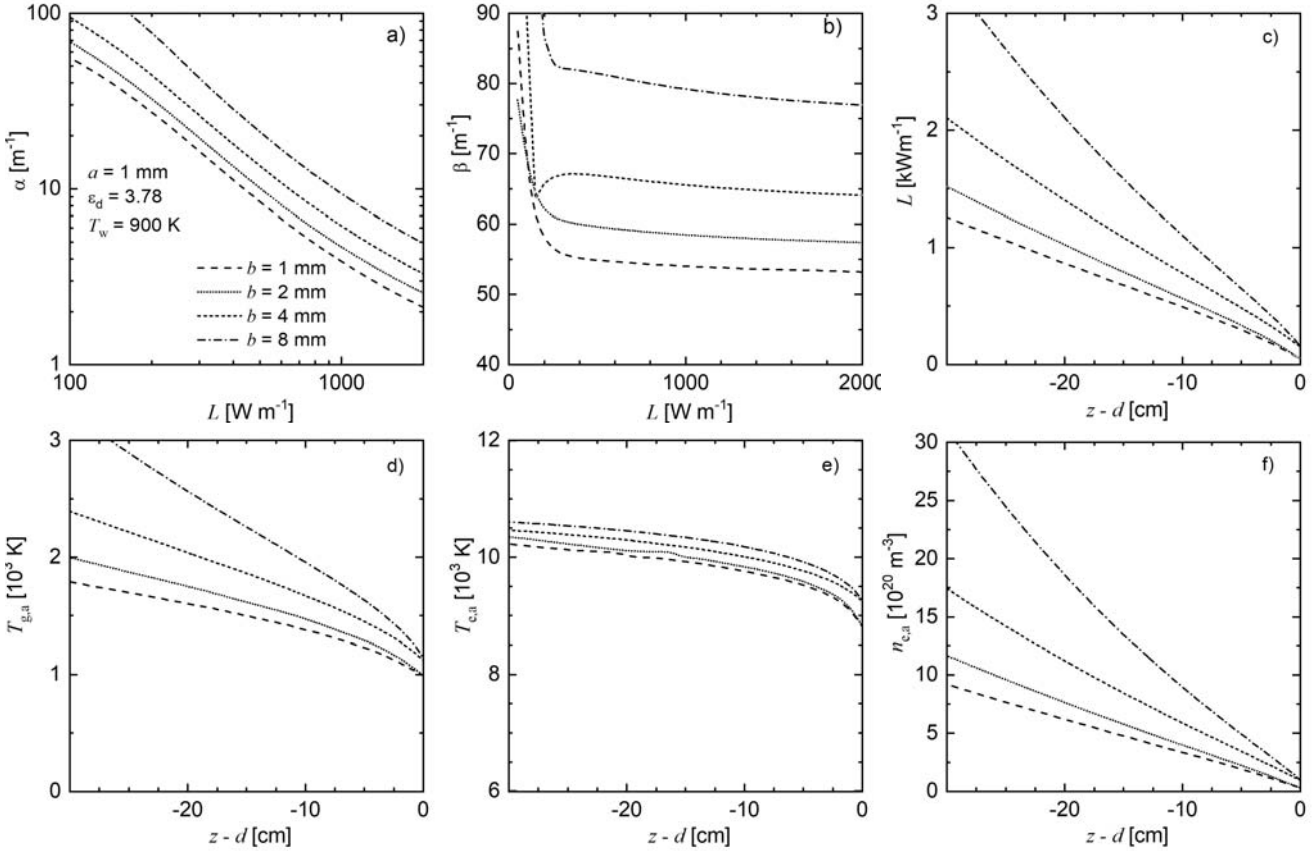

Fig.4. Influence of the discharge tube outer radius b on: a) SW attenuation characteristics $\alpha(L)$; b) SW phase characteristics $\beta(L)$; c) axial distribution of L, d) axial distributions of the average gas temperature Tg,a;, e) average electron temperature $T_{e,a}$, (f) average electron density $n_{e,a}$; T_w = 900 K, ε_d = 3.78, a = 1 mm

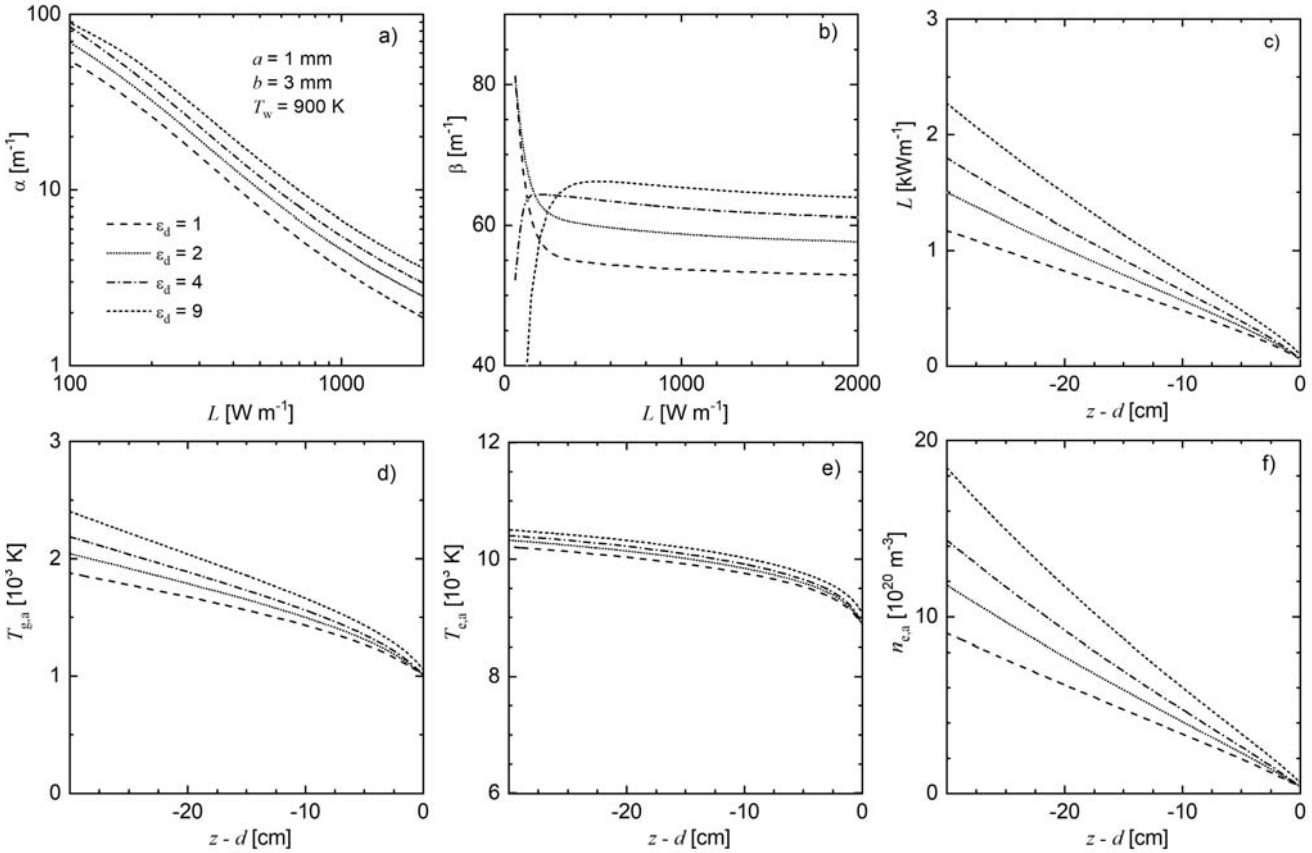

Fig.5. Influence of the discharge tube permittivity ε_d on: a) SW attenuation characteristics $\alpha(L)$; b) SW phase characteristics $\beta(L)$; c) axial distribution of L, d) axial distributions of the average gas temperature Tg,a, e) average electron temperature $T_{e,a}$, f) average electron density $n_{e,a}$; T_w = 900 K, a = 1 mm, b = 3 mm

Effect of the discharge tube wall temperature on the discharge parameters. The tube wall temperature T_w is the parameter used as the boundary condition for (3). In principle, it is not imposed in experiments. It results from the heating and cooling intensity of the tube and the gas flow rate and can be different in each experiment. In reduced-pressure discharge models, a value of 300 K was usually assumed. In atmospheric pressure models, it was often 700 K [13] or 900 K [17, 19]. It is worth noting that for given experimental conditions, it should be expected that this value changes along the tube. It is because the gas temperature at the inlet is about 300 K and along the discharge the gas is heated and the tube heats up from the gas.

Figs 6a and 6b show the influence of T_w on $\alpha(L)$ and $\beta(L)$, respectively. It seen that the higher T_w , the lower are both coefficients. The relationship $L(z)$ is almost linear and the slope of the curves and the values are greater for lower T_w. The increase in temperature T_w corresponds to the increase in the average gas temperature (Fig. 6d) in a selected discharge cross-section. A change of T_w from 500 to 1100 K causes a change in the average gas temperature from 800 to 1200 K at the end of the plasma column, and from 1900 to 2050 K (about 8%) at a distance of 30 cm from the plasma column end. It can be seen that the electron temperature (Fig. 6e) only weakly depends on T_w. Contrary to the gas temperature, it decreases with increasing T_w.

As in all previous cases, the electron density $n_{e,a}$ decreases almost linearly along the axis (Fig. 6f). Although it may seem strange that these values decrease with increasing T_w, this is due to the fact that $T_{e,a}$ also decreases with increasing T_w, and the ionization coefficient in (4) is an exponential function of the electron temperature. The impact of this parameter is not strong; however it may influence the explanation of the differences between the models and the experiment.

To our knowledge, the effect of T_w on plasma parameters has not been analyzed so far.

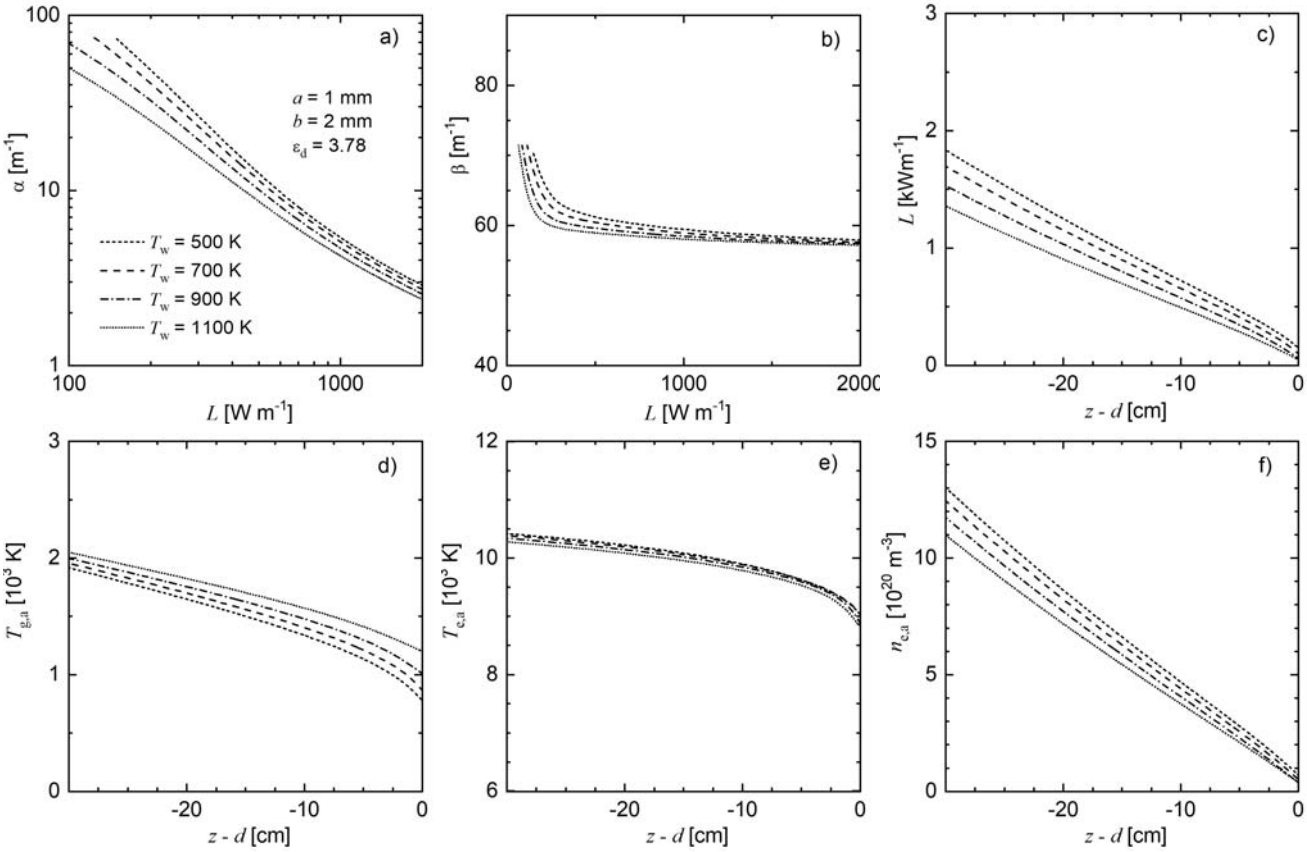

Figure 6. Influence of the discharge tube temperature T_w on: a) SW attenuation characteristics $\alpha(L)$; b) SW phase characteristics $\beta(L)$; c) axial distribution of L, d) axial distributions of the average gas temperature Tg,a, e) average electron temperature $T_{e,a}$, f) average electron density $n_{e,a}$; a = 1 mm, b = 3 mm, ε_d = 3.78

Summary and conclusion

This article presents the results of a systematic parametric study of the discharge tube properties the on the parameters of the plasma generated in a surface wave sustained discharge in argon at atmospheric pressure and wave frequency of 2.45 GHz, using the 2T LAUA model.

The influence of the discharge tube inner and outer radii, its permittivity and temperature on dependences of wave phase and attenuation coefficients on linear power density and on the axial distributions of the gas temperature, electron temperature and density are investigated.

In all analyzed cases, the dependence of attenuation coefficient on linear power density, $\alpha(L)$, is approximately a power function, and the axial distributions of L and $n_{e,a}$ are approximately linear functions.

The calculations show that the increase in the tube inner radius (while keeping the other parameters constant) reduces the wave phase and attenuation coefficients, the gas temperature, electron temperature and density as well as the slope of the curves $n_{e,a}(z-d)$ and $L(z-d)$.

Increasing the tube outer radius increases the wave propagation and attenuation coefficients, the gas temperature, electron temperature and density as well as the slope of the curves $n_{e,a}(z-d)$ and $L(z-d)$.

Increasing the permittivity of the tube (while keeping its radii constant) increases the wave phase and attenuation coefficients, the gas temperature, electron temperature and density as well as the slope of the curves $n_{e,a}(z-d)$ and $L(z-d)$. The effect on electron temperature is weak. For higher values of ε_d, a backward wave appears.

Increasing the tube wall temperature decreases the wave phase and attenuation coefficients, increases the gas temperature. It also slightly decreases the electron temperature, and as a result decreases also the electron density. The phase and attenuation coefficients depend mainly on the electron density, so they behave as it does

The results of systematic analysis of the influence of the discharge tube parameters presented in this paper provide insight into the behavior of discharges and facilitate their optimization. They may be useful for the analysis of experimental results and provide inspiration for more accurate models.

This research was funded by the Institute of Fluid Flow Machinery, Polish Academy of Sciences under the program IMP PAN O3/Z1/T1.

***Authors**: dr hab. inż. Helena Nowakowska, Instytut Maszyn Przepływowych im. Roberta Szewalskiego PAN, ul. Fiszera 14, 80-952 Gdańsk, E-mail: helena.nowakowska@imp.gda.pl*

REFERENCES

[1] Moisan M., Zakrzewski Z., Pantel R., The theory and characteristics of an efficient surface wave launcher (surfatron) producing long plasma columns, *J Phys Appl Phys* 12 (1979), 219–37

[2] Moisan M., Glaude V., Leprince P., Mitchel G., Zakrzewski Z., Surfaguide - waveguide plasma source using surface-waves, *Bulletin of the American Physical Society*, 21 (1976), 812–812

[3] Kabouzi Y., Moisan M., Rostaing J-C., Trassy C., Guerin D., Keroack D., Zakrzewski Z., Abatement of perfluorinated compounds using microwave plasmas at atmospheric pressure, *J Appl Phys* 93 (2003), No. 12, 9483–96

[4] Muñoz J., Rincón R., Calzada MD., Spatial Distribution of Wettability in Aluminum Surfaces Treated with an Atmospheric-Pressure Remote-Plasma, *Metals* 9 (2019), No. 9, 937

[5] Chen G., Silva T., Georgieva V., Godfroid T., Britun N., Snyders R., Delplancke-Ogletree MP., Simultaneous dissociation of CO_2 and H_2O to syngas in a surface-wave microwave discharge, *Int J Hydrog Energy* 40 (2015), No. 9, 3789–96

[6] Casanova A., Rincón R., Muñoz J., Ania CO., Calzada MD., Optimizing high-quality graphene nanoflakes production through organic (bio)-precursor plasma decomposition, *Fuel Process Technol* 212 (2021), 106630(12)

[7] de la Fuente JF., Moreno SH., Stankiewicz AI., Stefanidis GD., On the improvement of chemical conversion in a surface-wave microwave plasma reactor for CO_2 reduction with hydrogen (The Reverse Water-Gas Shift reaction), *Int J Hydrog Energy* 42 (2017), No. 18, 12943–55

[8] Sadeghikia F., Talafi Noghani M., Simard MR., Experimental study on the surface wave driven plasma antenna, *AEU - Int J Electron Commun* 70 (2016), No. 5, 652–6

[9] Moisan M., Nowakowska H., Contribution of surface-wave (SW) sustained plasma columns to the modeling of RF and microwave discharges with new insight into some of their features. A survey of other types of SW discharges, *Plasma Sources Sci Technol* 27 (2018), No. 7, 073001(43)

[10] Glaude VMM., Moisan M., Pantel R., Leprince P., Marec J., Axial electron density and wave power distributions along a plasma column sustained by the propagation of a surface microwave, *J Appl Phys* 51 (1980), No. 11, 5693–8

[11] Zhelyazkov I., Benova E., Modeling of a plasma column produced and sustained by a traveling electromagnetic surface wave, *J Appl Phys* 66 (1989), No. 4, 1641–50

[12] Zhelyazkov I., Atanassov V., Axial structure of low-pressure high-frequency discharges sustained by travelling electromagnetic surface waves, *Phys Rep* 255 (1995), No. 2–3, 79–201

[13] Kabouzi Y., Graves DB., Castaños-Martínez E., Moisan M., Modeling of atmospheric-pressure plasma columns sustained by surface waves, *Phys Rev E* 75 (2007), No. 1, 016402(14)

[14] Georgieva V., Berthelot A., Silva T., Kolev S., Graef W., Britun N. et al., Understanding Microwave Surface-Wave Sustained Plasmas at Intermediate Pressure by 2D Modeling and Experiments, *Plasma Process Polym* 14 (2017), No. 4–5, 1600185(25)

[15] Tebani H., A global model for the inductively coupled rf discharges in Ar/H_2 mixture, *Przegląd Elektrotechniczny* 1 (2021), No. 1, 32–8

[16] Kemaneci E., Mitschker F., Rudolph M., Szeremley D., Eremin D., Awakowicz P., Peter Brinkmann R., A global model of cylindrical and coaxial surface-wave discharges, *J Phys Appl Phys* 50 (2017), No. 24, 245203

[17] Castaños Martinez E., Kabouzi Y., Makasheva K., Moisan M., Modeling of microwave-sustained plasmas at atmospheric pressure with application to discharge contraction, *Phys Rev E* 70 (2004), No. 6, 066405(12)

[18] Nowakowska H., Czylkowski D., Zakrzewski Z., Surface wave sustained discharge in argon: two-temperature collisional-radiative model and experimental verification, *J Optoelectron Adv Mater* 7 (2005), No. 5, 2427–34

[19] Nowakowska H., Jasiński M., Mizeraczyk J., Modelling of discharge in a high-flow microwave plasma source (MPS), *Eur Phys J D* 67 (2013), No. 7, 133(8)

[20] Jimenez-Diaz M., Carbone EAD., van Dijk J., van der Mullen JJAM., A two-dimensional Plasimo multiphysics model for the plasma–electromagnetic interaction in surface wave discharges: the surfatron source, *J Phys Appl Phys* 45 (2012), No. 33, 335204

[21] Christova M., Castaños-Martinez E., Calzada MD., Kabouzi Y., Luque JM., Moisan M., Electron Density and Gas Temperature from Line Broadening in an Argon Surface-Wave-Sustained Discharge at Atmospheric Pressure, *Appl Spectrosc* 58 (2004), No. 9, 1032–7

[22] Sáinz A., García MC., Calzada MD., Spectroscopic determination of the electron temperature in non-LTE argon and neon plasmas, *2005 ECA Vol. 29C, P-4.132*. Tarragona (2005)

[23] Durocher-Jean A., Desjardins E., Stafford L., Characterization of a microwave argon plasma column at atmospheric pressure by optical emission and absorption spectroscopy coupled with collisional-radiative modelling, *Phys Plasmas* 26 (2019), No. 6, 063516(13)

[24] Castaños-Martínez E., Moisan M., Kabouzi Y., Achieving non-contracted and non-filamentary rare-gas tubular discharges at atmospheric pressure, *J Phys Appl Phys* 42 (2009), No. 1, 012003(5)

[25] Ridenti MA., de Amorim J., Dal Pino A., Guerra V., Petrov G., Causes of plasma column contraction in surface-wave-driven discharges in argon at atmospheric pressure, *Phys Rev E* 97 (2018), No. 1, 013201(14)

[26] Kovačević MS., Kuzmanović L., Milošević MM., Djordjevich A., An estimation of the axial structure of surface-wave produced plasma column, *Phys Plasmas* 28 (2021), No. 2, 023502(5)

[27] Chen C-J., Li S-Z., Wu Y., Zhang J., Investigation of role of the discharge tube in pulse modulated surface-wave argon plasma column at atmospheric pressure by optical emission spectroscopy, *Phys Plasmas* 26 (2019), No. 5, 053506

[28] Fujiwara K., Endo M., Ikeda Y., Suzuki T., Yanagisawa M., Shindo H., Radio-Frequency Downstream Plasma Production by Surface-Wave in a Very High-Permittivity Material Discharge Tube, *Jpn J Appl Phys* 44 (2005), No. 15, L457–60